Utilization of biomass fly ash in alkali-activated materials

Liang, X.; Dong, H.; Li, Z.; van Zijl, Marc Brito; Ye, G.

Publication date
2021

Document Version
Final published version

Published in
4th International Rilem Conference on Microstructure Related Durability of Cementitious Composites

UTILIZATION OF BIOMASS FLY ASH IN ALKALI-ACTIVATED MATERIALS

Xuhui Liang (1), Hua Dong (1), Zhenming Li (1), Marc Brito van Zijl (2), and Guang Ye (1)

(1) Section of Materials and Environment (Microlab), Faculty of Civil Engineering and Geoscience, Delft University of Technology, Delft, the Netherlands

(2) Mineralz, Loswalweg 50, Rotterdam, the Netherlands

Abstract

This paper investigated the feasibility of using biomass fly ash (BFA) to prepare alkali-activated slag and fly ash paste. The reference mixture was alkali-activated slag and coal fly ash (CFA) paste with a slag-to-coal fly ash ratio of 50/50. In other mixtures, coal fly ash was replaced at 40% and 100% with BFA, respectively. The results showed that the incorporation of BFA accelerated the setting of the paste, while its impact on the compressive strength was minor. XRD and FTIR results indicated that the BFA participated in the reaction process. BFA showed potential use as CFA replacement in synthesizing alkali-activated materials, which would pave a way for the valorisation of BFA.

Keywords: biomass fly ash, alkali-activated materials, waste

1. INTRODUCTION

Fossil fuels are currently the most dominant resource for energy production. Besides the high expenses and irreversibility of fossil fuels, their burning process releases a large quantity of greenhouse gases, causing negative impact on the environment [1]. It has been agreed that by 2030, EU shall reduce the CO_2 emission by 40%. The energy industries take great responsibility and have to shift their focus to clean energy [2]. Thus, the desire for alternative fuels is greater than ever before. Bioenergy, derived from the biomass incineration, stands out for its superior characteristics with cheap resources and minor environmental impact. It is believed that biomass is carbon-neutral fuel, where CO_2 emissions during biomass combustion could be compensated through photosynthesis process [3, 4]. Therefore, the biomass is praised with bright prospects. Up to now, biomass has been applied as the fourth most used fuels for energy production, contributing to 10-14 % of total energy production worldwide [5, 6]. It is proposed that an increasing amount of biomass will be used in the coming decades [2].

During the incineration process of biomass for bioenergy production, by-products will be generated. Biomass fly ash (BFA) is the main residue from incineration process. The unburnt fine particles are carried by flue gas and eventually collected through bag filters or electrostatic

filters. Currently, most of BFA is landfilled or disposed directly, resulting in serious environmental problems. Recycling BFA and using it in building materials will benefit the environment and prompt the development of clean bioenergy. However. BFA is prohibited to be used in Portland cement concrete according to EN 450-1 [7], which requires the fly ash for concrete use should derived from coal combustion.

Apart from Portland cement, alkali-activation could be a possible way for BFA valorisation. Alkali-activated materials (AAM) is one type of cement clinker free binder and a promising alternative to Portland cement [8]. In recent years, intensive investigations have been carried out on AAMs. AAMs have high compatibility with raw materials [8]. Multiple industrial aluminosilicates wastes were used as precursors for AAMs preparation [9-12]. AAMs made of blast furnace slag (BFS) and coal fly ash (CFA) have shown good mechanical properties and workability [13, 14]. However, studies on BFA in AAM are scarce. The aim of this paper, therefore, is to investigate the possibilities of using BFA as precursor for producing AAM, where the BFA was used to partially replace the coal fly ash in alkali-activated slag and fly ash system.

2. MATERIALS AND METHODS

2.1 Materials

Biomass fly ash was collected from an energy plant in the Netherlands, where multiple biomass was used as fuel. Ground granulated blast furnace slag (GGBFS) and CFA were supplied by Ecocem Benelux BV (the Netherlands) and Vliegasunie BV (the Netherlands), respectively.

The particle size distribution of the raw materials was measured by laser diffraction analyser (DIPA 2000). Particle sizes of BFA were all below than 55 μm and close the GGBFS, while CFA showed bigger particle sizes, as shown in Fig. 1. The chemical and mineralogical compositions were determined through X-ray fluorescence (XRF) and X-ray diffraction (XRD), respectively.

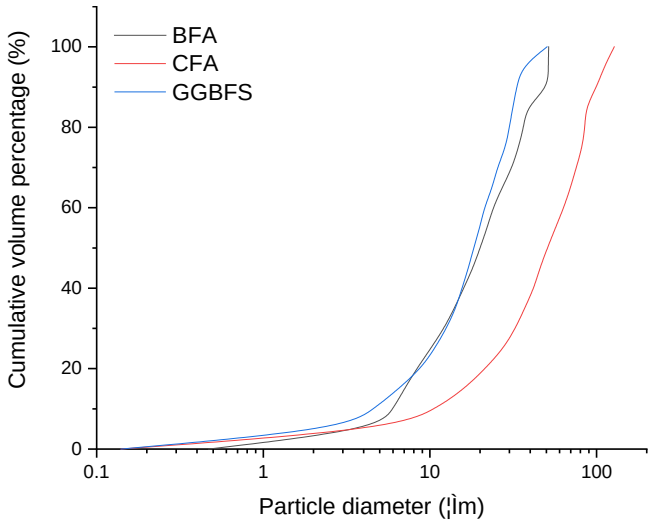

Figure 1: Particle size distribution of raw materials

According to the chemical composition, BFA contained higher amount of calcium oxide (CaO) compared with CFA (Tab. 1), and can be regarded as the Class C fly ash. The XRD pattern of BFA was almost flat with crystalline peaks, showing minor amount of glassy phases. There was a broad hump between 20-30 degrees for CFA, which represented the amorphous phases. The slag consisted of typical glassy phases almost without crystalline phases.

Table 1 Chemical composition of raw materials

	SiO_2	Al_2O_3	CaO	Fe_2O_3	K_2O	SO_3	Na_2O	Cl
BFA	50.92	12.53	17.16	7.70	2.18	3.77	0.27	0.12
CFA	52.60	26.37	5.46	9.52	1.55	0.85	-	-
BFS	32.19	13.43	41.04	0.52	0.34	1.51	-	-

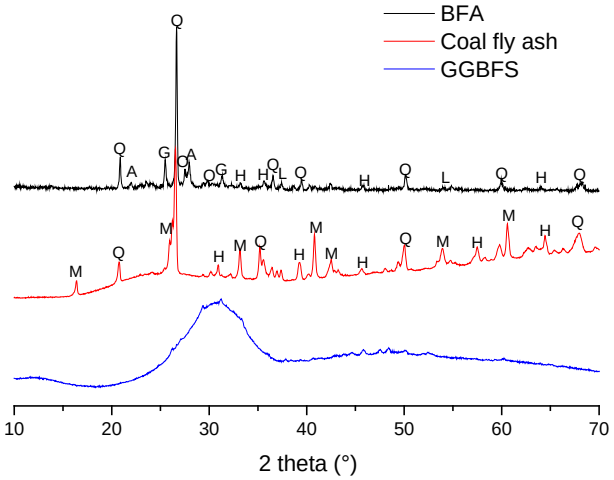

Figure 2: XRD patterns of raw materials
(Q: quartz, M: mullite, H: hematite A: albite, O: orthoclase, G: gypsum, L: lime)

The alkaline activator was a mix of sodium hydroxide (analytical reagent, >98% purity) and water glass solution (Na_2O: 8.25 wt%, SiO2: 27.50 wt%). The molar ratio of SiO_2 to Na_2O of the activator was 1.5 and the mass ratio of Na_2O to binder was 4.5%.

2.2 Methods

Three kinds of alkali-activated paste were prepared with the mixture proportion shown in Tab 2. All the raw materials were premixed in the mixer for 2 min to reach a homogenous state, then the activator was gradually added and the mixing continued for another 2 min. The paste was cast into cubes ($4 \times 4 \times 4$ cm^3) and compacted on the vibration table. Afterwards, the specimens were covered with plastic films to avoid water evaporation. Specimens were demoulded after one day, sealed in plastic bags and placed in the curing room at 20 ^oC until the compressive strength tests [15].

Table 2: Mixture proportion of alkali-activated slag and fly ash paste

Mixture	BFS(.wt%)	CFA(.wt%)	BFA(.wt%)	Liquid/Solid
B0	50	50	0	0.5
B20		30	20	
B50		0	50	

Setting time was determined using an automatic Vicat apparatus (VICAMATIC 2). The experiment was conducted at 20 ºC and 50 % RH following EN 196-3 [16]. Isothermal calorimetry test was carried out to study the hydration process of pastes at 20 ºC. Compressive strength test was conducted at a loading speed of 2.4 kN/s following EN 196-1 [17]. Five specimens were tested for each mixture, and the average compressive strength was calculated. After the compression tests, interior fragments of the specimens were collected and subjected to grinding and hydration stoppage for XRD and FTIR tests. The procedures for hydration stoppage could be found in ref [18].

XRD technique was applied to study the characteristics of hydration products in different pastes. Powder samples were prepared and their XRD patterns were determined by Philips X'Pert diffractometer. Scanning was conducted with Cu Kα radiation, the 2 theta increased from 10 º to 70º with a step size 0.03º. FT-IR (Spectrum TM 100 Optical ATR-FTIR) was applied for measuring the chemical bonds of molecules in raw materials and hydration products.

3. RESULTS AND DISCUSSION

3.1 Setting time and calorimetry

The setting time of the pastes was shown in Tab 3. It shows that the initial and the final setting time decreased with the increasing amount of BFA.

Table 3: Setting time of the pastes

Mixture	Initial setting (min)	Final setting (min)
B0	51	86
B20	29	57
B50	16	35

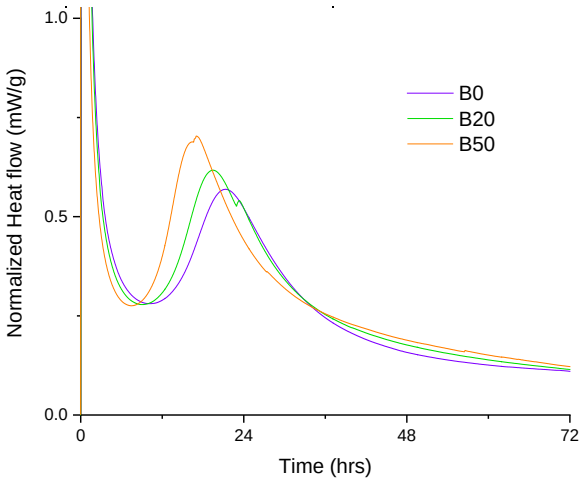

Figure 3: Heat flow of the pastes

It is believed that setting time could be linked to the hydration rate of early age pastes. Shorter setting time indicates faster chemical reaction in the pastes. The reasons for the acceleration of hydration can be explained by two facts. 1). From the chemical composition point of view, the amount of calcium in BFA is higher than that in coal fly ash. When mixed with alkaline solution, a higher amount of calcium in BFA would be released, which was beneficial for C-(A)-S-H precipitation [19]. 2). The finer particles of BFA have a nucleation effect and account for the faster setting [20].

Fig 3 presents the heat realise rate of pastes. The first peak in the heat release curve is related to the dissolution of precursors, and the second peak is for the formation of reaction products. With the incorporation of BFA, the second peak appeared earlier with higher intensity, which suggested an accelerated formation of C-(A)-S-H gel at early stage.

3.2 Compressive strength

The compressive strength of alkali-activated slag and coal/biomass fly ash at 1d and 7d was shown in Fig 4. Despite the acceleration of hydration, the incorporation of BFA did not improve the compressive strength at 1d. The compressive strength at 1d of all specimens was close to 20 MPa. With the proceeding hydration, the strength increased to nearly 65 MPa at 7d. A slight improvement of compressive strength was observed with the incorporation of BFA.

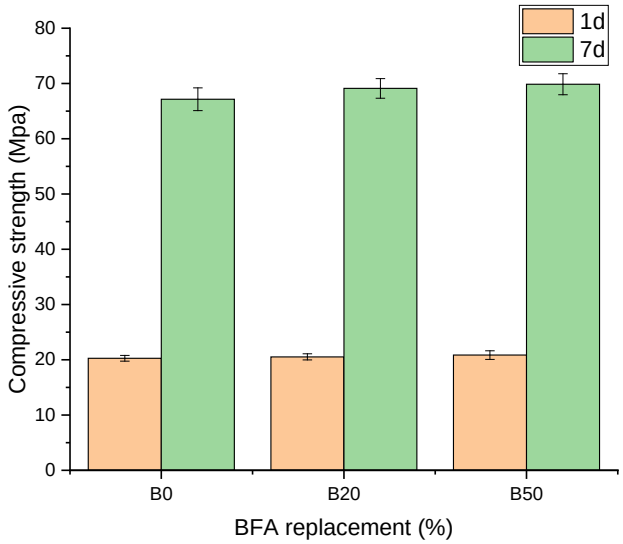

Figure 4: Compressive strength of alkali-activated slag and coal/biomass fly ash

3.3 XRD analysis

The XRD results of B50 at 1 day and 7 days, and B0 at 7 days were shown in Fig 5. Unreactive phases such as quartz and hematite, etc. remained in the XRD patterns after 1 and 7 d of reaction in B50 samples. It can be found that the peak at 2 theta angle of 25.5^{o}, which represents anhydrite in BFA, disappeared after alkali activation. The intensity of peaks at 2-theta angle of 28^{o} representing albite comparatively decreased from 1d to 7d. These could be explained by the dissolution of BFA in alkaline solution. Meanwhile, XRD spectrum for all samples presented a peak at 2 theta angle of around 29^{o}, which is associated with the formation of C-(A)-S-H gel [21]. The intensity of C-(A)-S-H peak in B50 increased from 1d to 7d, indicating more reaction products were formed, which contributed to the strength development.

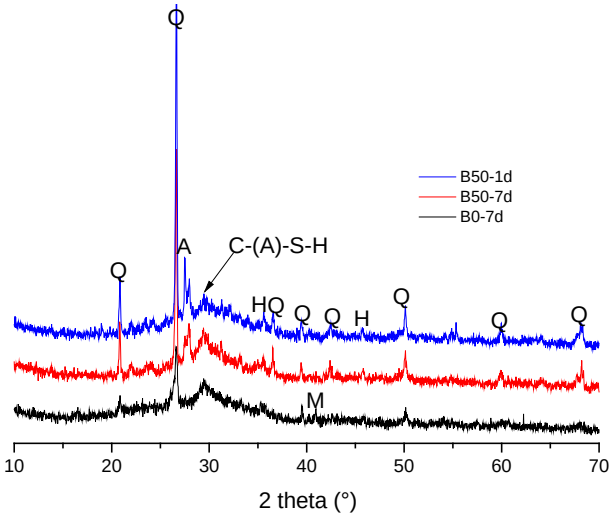

Figure 5: XRD patterns of hardened paste (Q: quartz, M: mullite, H: hematite A: albite)

3.4 FT-IR analysis

Fig 6 showed the FT-IR spectra of CFA, BFA, B0 at 7d and B50 at 7d. For CFA and BFA, the main bands around 1100 cm^{-1} were related with Si(Al)-O-Si [22, 23]. The tiny difference in wavenumbers at the main band (1097^{-1} and 1050 cm^{-1}) between CFA and BFA was the results of aluminium substitution in silicon tetrahedral position [23, 24]. Calcium sulphate was also observed for BFA at 678 cm^{-1} and 611 cm^{-1}, in agreement with the XRD results of the presence of anhydrite. Broad bands presented at 3400 cm^{-1} and 1625 cm^{-1} in B0-7d and B50-7d samples represented the vibration of hydroxyl (water) [22]. The main band at 945 cm^{-1} indicated the existence of C-(A)-S-H, which was the dominant hydration products for both B0 and B50 [25]. Generally, the spectrums for hydration products in B0 and B50 were similar. The band representing sulphate in the raw materials BFA disappeared after hydration, which confirmed that the sulphate dissolved in alkali activation and participated in reaction process.

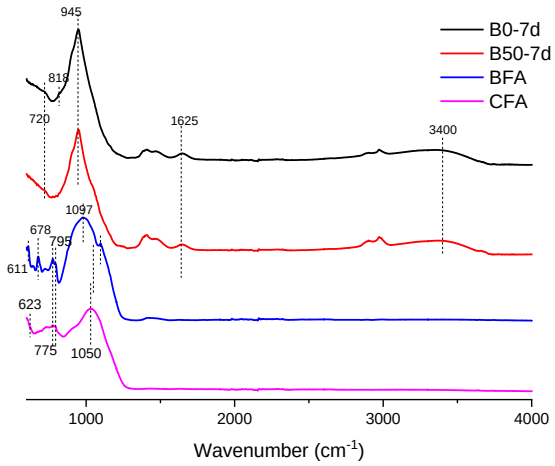

Figure 6: FT-IR spectra of precursors and pastes

4 CONCLUSIONS

Based on the results, the following conclusions can be drawn:

- Due to the high soluble calcium salts and fine particle size of BFA, the incorporation of BFA accelerated the setting of alkali-activated slag and fly ash paste, while showing minor impact on compressive strength at early age.
- BFA could dissolve in alkaline activation, which was confirmed through the dissolution of anhydrite, lime and albite determined through XRD and FTIR.
- BFA showed potential as a precursor for synthesizing alkali activated materials, which could be a promising routine for its valorisation.

ACKNOWLEDGEMENT

Xuhui Liang acknowledges the financial support from China Scholarship Council (No.201806050051). Zhenming Li acknowledges the financial support from China Scholarship Council (No.201506120072). Mineralz was acknowledged for the financial support of the experiments.

REFERENCES

1. Energy, I.G., *Global Energy & CO_2 Status Report: The Latest Trends in Energy and Emissions in 2018.* International energy agency iea, 2019: p. 1.
2. Commission, E.E., *GREEN PAPER-a 2030 framework for climate and energy policies.* COM (2013), 2013. **169**.
3. Agrela, F., et al., *2 - Biomass fly ash and biomass bottom ash*, in *New Trends in Eco-efficient and Recycled Concrete*, J. de Brito and F. Agrela, Editors. 2019, Woodhead Publishing. p. 23-58.
4. Johnson, E., *Goodbye to carbon neutral: Getting biomass footprints right.* Environmental Impact Assessment Review, 2009. **29**(3): p. 165-168.
5. McKendry, P., *Energy production from biomass (part 1): overview of biomass.* Bioresource Technology, 2002. **83**(1): p. 37-46.
6. Islas, J., et al., *Chapter Four - Solid Biomass to Heat and Power*, in *The Role of Bioenergy in the Bioeconomy*, C. Lago, N. Caldés, and Y. Lechón, Editors. 2019, Academic Press. p. 145-177.
7. EN, B., *450-1, Fly Ash for Concrete—Definition, Specifications and Conformity Criteria.* British Standards Institution, 2012.
8. Provis, J.L., *Alkali-activated materials.* Cement and Concrete Research, 2018. **114**: p. 40-48.
9. Fořt, J., et al., *Application of waste brick powder in alkali activated aluminosilicates: Functional and environmental aspects.* Journal of Cleaner Production, 2018. **194**: p. 714-725.
10. Palmero, P., et al., *Valorisation of alumino-silicate stone muds: From wastes to source materials for innovative alkali-activated materials.* Cement and Concrete Composites, 2017. **83**: p. 251-262.
11. He, J., et al., *Synthesis and characterization of red mud and rice husk ash-based geopolymer composites.* Cement and Concrete Composites, 2013. **37**: p. 108-118.

12. Bernal, S.A., et al., *Management and valorisation of wastes through use in producing alkali-activated cement materials.* Journal of Chemical Technology & Biotechnology, 2016. **91**(9): p. 2365-2388.
13. Nedeljković, M., Z. Li, and G. Ye, *Setting, Strength, and Autogenous Shrinkage of Alkali-Activated Fly Ash and Slag Pastes: Effect of Slag Content.* Materials, 2018. **11**(11): p. 2121.
14. Yousefi Oderji, S., et al., *Fresh and hardened properties of one-part fly ash-based geopolymer binders cured at room temperature: Effect of slag and alkali activators.* Journal of Cleaner Production, 2019. **225**: p. 1-10.
15. Nedeljković, M., et al., *Effect of curing conditions on the pore solution and carbonation resistance of alkali-activated fly ash and slag pastes.* Cement and Concrete Research, 2019. **116**: p. 146-158.
16. BSI, *BS EN 196-3: Methods of testing cement–Part 3: Determination of setting times and soundness*. 2005, BSI London, UK.
17. EN, T., *196-1. Methods of testing cement–Part 1: Determination of strength.* European Committee for standardization, 2005. **26**.
18. Snellings, R., et al., *RILEM TC-238 SCM recommendation on hydration stoppage by solvent exchange for the study of hydrate assemblages.* Materials and Structures, 2018. **51**(6): p. 172.
19. Song, W., et al., *Effect of steel slag on fresh, hardened and microstructural properties of high-calcium fly ash based geopolymers at standard curing condition.* Construction and Building Materials, 2019. **229**: p. 116933.
20. Scrivener, K.L., P. Juilland, and P.J.M. Monteiro, *Advances in understanding hydration of Portland cement.* Cement and Concrete Research, 2015. **78**: p. 38-56.
21. Zuo, Y., M. Nedeljković, and G. Ye, *Pore solution composition of alkali-activated slag/fly ash pastes.* Cement and Concrete Research, 2019. **115**: p. 230-250.
22. Zhang, Z., H. Wang, and J.L. Provis, *Quantitative study of the reactivity of fly ash in geopolymerization by FTIR.* Journal of Sustainable Cement-Based Materials, 2012. **1**(4): p. 154-166.
23. Mozgawa, W., et al., *Investigation of the coal fly ashes using IR spectroscopy.* Spectrochimica Acta Part A: Molecular and Biomolecular Spectroscopy, 2014. **132**: p. 889-894.
24. Flanigen, E.M., H. Khatami, and H.A. Szymanski, *Infrared Structural Studies of Zeolite Frameworks*, in *Molecular Sieve Zeolites-I*. 1974, AMERICAN CHEMICAL SOCIETY. p. 201-229.
25. Li, Z., et al., *Mitigating the autogenous shrinkage of alkali-activated slag by metakaolin.* Cement and Concrete Research, 2019. **122**: p. 30-41.